

# A Hybrid DC-DC Converter for Standalone Applications

Varun Jo Abu<sup>1</sup>, Sija Gopinathan<sup>2</sup>, Leela Salim<sup>3</sup>

<sup>1</sup>PG Scholar, Department of Electrical and Electronics Engineering, Mar Athanasius College of Engineering, Kothamangalam, Kerala, India

<sup>2</sup>Assistant Professor, Department of Electrical and Electronics Engineering, Mar Athanasius College of Engineering, Kothamangalam, Kerala, India

<sup>3</sup>Assistant Professor, Department of Electrical and Electronics Engineering, Mar Athanasius College of Engineering, Kothamangalam, Kerala, India

\*\*\*

**Abstract** - The conventional energy sources available in the world are diminishing every year creating a huge difference between the demanded energy and the available energy. Efficient utilization of the ample renewable energy resources present in the world can be used to cover this extra demand. With the use of this renewable energy sources the levels of pollution and global warming can be controlled to a lower level. A significant demerit with the renewable energy sources is their fluctuating nature. Hybridization technique is hence utilized to overcome this problem. This allows two sources to meet the load separately or simultaneously depending on the availability. In this paper a double input single output DC-DC converter is presented for stand-alone systems. The topology operates as a bootstrap circuit by employing the charging switches in case of only one input port powering or one input being short circuited and maintains the expected output voltage making the system fault tolerant.

**Key Words:** Hybrid system, Multi-input converter, Bootstrap operation, Solar panel, Fuel cell

## 1. INTRODUCTION

Rise in the energy demand and limitation in fossil fuels have increased the role of renewable energy resources. Renewable energy sources will have to play a significant role in overcoming these problems. Systems based on petroleum product and fossil fuels will result in environmental pollution and hence global warming. This elevated the need for renewable energy sources which is abundant and environment friendly. Solar energy, wind energy, etc. are capable of supplying energy to meet the power demand. Even though the capital cost and space requirement for such systems are high, the running cost is extremely low. They can be easily utilized in distributed generation, micro grid, stand-alone systems, rural telephony systems etc. The main disadvantage of such a system is its unpredictable and intermittent nature, i.e., the output from these systems will always be fluctuating and doesn't deliver a constant output. To overcome this challenge, hybrid renewable energy systems were implemented which club two or more energy resources to produce a constant output. Hybridization improves the efficiency and life of the system and also brings down the storage requirement. However, by combining these

two fluctuating sources, the efficiency and reliability of the system can be refined notably. At the same time, the capital cost and complexity can increase as a result of hybridization.

Multi input converters (MIC) have a simpler structure, improved power density and lower cost due to sharing of switches and other components [1]-[3]. Dynamic performance can be improved and complex communication among multiple different sources can be avoided due to the unified power management with centralized control. Thus MIC is appropriate for renewable power systems. Isolated [4]-[6] and non-isolated MIC has been developed for DC-DC conversion. Galvanic isolation is used in isolated MICs, but the disadvantage is the larger number of active switches present in it. Non-isolated converters have the advantages of small size, high power density and more efficiency. Based on buck and/or boost converter structures, various non-isolated topologies were developed. A triple input boost DC-DC converter developed in [7] consists of a photovoltaic source, fuel cell and a battery in a unified structure. A buck voltage source cell parallel connected MIC is presented in [8] which can operate in buck, boost or buck-boost mode, but with only any one of the input ports powering. Two-input series-connected buck DC-DC converters proposed in [9]-[11] have a simple topology and efficient energy utilization. They can deliver power to the load from two power sources simultaneously or individually. The series-connected two-input converter in [10] has one input port connected to a renewable energy source and other to a storage element, used for nanogrid application. Although both individual and simultaneous operations are possible for this converter, when one input source is shut down, the other port takes up the operation and the output voltage will be less than the existing input voltage. This implies that the converter is not able to maintain the expected output voltage in the one port powering case if the expected output voltage is more than either of two input voltages.

Due to the randomness and intermittency of renewable energy sources present as inputs, it is necessary for the converter to be loaded with a flexible compensation program for error free individual operation. A circuit topology was designed in [12] which include a combination of a charging switch and a series connected double input converter (SCDIC). In this circuit, the converter operates in bootstrap mode in the case of one port powering and it meets the expected output voltage. The disadvantage with this topology

is that it employs a large number of switches and hence the switching losses will be larger. But this topology has the merit of employing only a single inductor for any number of input ports when compared to parallel boost converters. This advantage will in turn reduce the volume and cost and improve the dynamic response of the system.

This paper proposes another series connected double input converter with reduced number of switches and possessing all the advantage of the circuit presented in [12]. With the presence of a blocking diode, the chance of fault due to a short circuited input can be ruled out. In such a case, the short circuit input port will be separated from the converter and the port will be powered by bootstrap operation.

The paper consists of four sections. After introduction in section I, the circuit features, principle and modes of operation will be described in section II. Section III presents the simulation model and results of the converter and section IV concludes the paper.

**Table -1:** Comparison of the proposed converter with SCDIC converter [12]

PARAMETER	SCDIC CONVERTER	PROPOSED CONVERTER
No. of inputs	2	2
No. of switches	6	5
No. of diodes	1	2

## 2. HYBRID DC-DC CONVERTER

A circuit diagram of the hybrid energy system is shown in figure 3, where one of the inputs is connected to the PV array and the other input is connected to a fuel cell.  $V_{in1}$  and  $V_{in2}$  are the two input source voltages.  $C_1$  is the bootstrap capacitor and is connected across  $V_{in1}$ .  $D_1$  is the blocking diode and it separates a short circuited input source from the converter. Switches  $S_4$  and  $S_5$  are the charging switches during bootstrap operation.  $L_f$  is the filter inductor,  $C_f$  is the filter capacitor and  $R_o$  is the load resistor. All the switches in the converter are MOSFETs. This configuration allows both individual and simultaneous operation of the converters. So the circuit can operate in three modes depending on the available inputs. The circuit has 6 states of operation. When both sources are unavailable the entire circuit will be turned off. Table 2 shows the modes of operation.

**Table -2:** Modes of operation

MODE	$V_{in1}$ (SOLAR SOURCE)	$V_{in2}$ (FUEL CELL)
I(Simultaneous operation)	ON	ON
II(Bootstrap operation)	OFF	ON
III	ON	OFF

Although modes I and II can occur in a practical situation, mode III has least chances to occur. Figure 1 shows the circuit diagram of the converter. States 1 and 2 is during the bootstrap operation mode, i.e., during the individual operation of  $V_{in2}$ . Rest of the states from 3-6 occurs at the remaining modes, i.e., during individual operation of  $V_{in1}$  or during simultaneous operation. The expected output voltage is kept above either of the two input voltages. Take  $V_{in1} > V_o > V_{in2}$ .

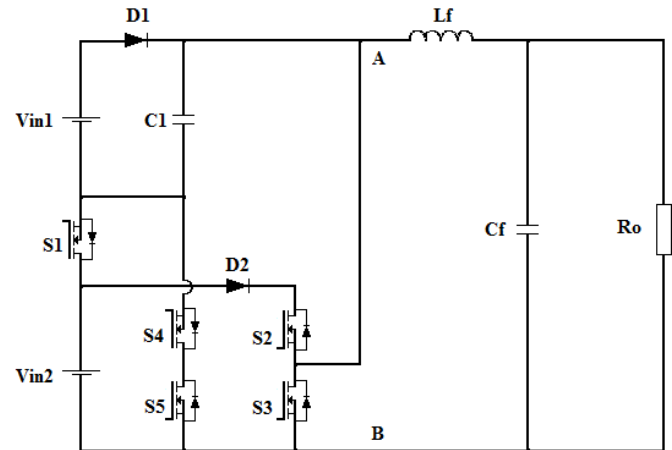


**Fig -1:** Circuit diagram of the hybrid DC-DC converter for standalone applications

**State I:** ( $S_2, S_4, S_5$  ON,  $S_1, S_3$  OFF)

$V_{in2}$  charges the capacitor  $C_1$  through the switches  $S_2, S_4$  and  $S_5$ . Now the voltage across the points A and B ( $v_{AB}$ ) will be  $V_{in2}$  and it is below  $V_o$ . Now the voltage appearing across the inductor  $L_f$  is negative and thereby the current  $i_{L_f}$  decreases. The power to load is supplied alone by  $V_{in2}$  in this state. Figure 2(a) shows the equivalent circuit during state I.

$$v_{AB} = V_{in2} \tag{1}$$

$$\frac{di_{L_f}}{dt} = \frac{V_{in2} - V_o}{L_f} \tag{2}$$

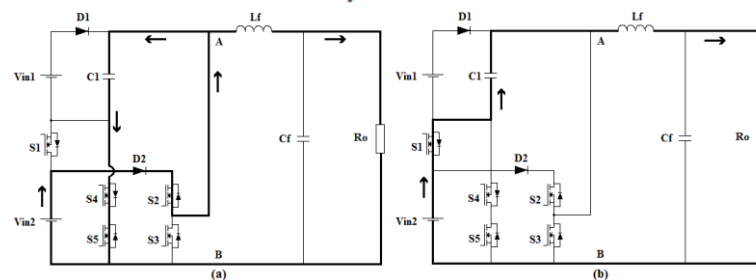


**Fig -2:** Equivalent circuit during (a) State I, (b) State II

**State II:** ( $S_1$  ON,  $S_2, S_3, S_4, S_5$  OFF)

$V_{in2}$  is now in series with the bootstrap capacitor  $C_1$ . Now the voltage across the points A and B ( $v_{AB}$ ) will be  $2V_{in2}$  and it is above  $V_o$ . This makes the voltage across the inductor  $L_f$  positive and thereby the inductor current  $i_{L_f}$  rises. Figure 2(b) shows the equivalent circuit during state II.

$$v_{AB} = 2V_{in2} \tag{3}$$

$$\frac{di_{L_f}}{dt} = \frac{2V_{in2} - V_o}{L_f} \quad (4)$$

It can be seen that when  $V_{in1}$  is powered off from its port, the port is taken up by  $V_{in2}$  through bootstrap operation and the expected output voltage is met. For the remaining states, both sources  $V_{in1}$  and  $V_{in2}$  are available and simultaneous operation of the converter takes place.

**State III:** ( $S_1$  ON,  $S_2, S_3, S_4, S_5$  OFF)

Sources  $V_{in1}$  and  $V_{in2}$  connected in series during this state to deliver the power to the load. The voltage across the points A and B ( $v_{AB}$ ) will be  $V_{in1} + V_{in2}$  and it is more than  $V_o$ . Now the voltage appearing across the inductor  $L_f$  is  $(V_{in1} + V_{in2} - V_o)$  and thereby the current  $i_{L_f}$  increases linearly. Figure 3(a) shows the equivalent circuit during state III.

$$v_{AB} = V_{in1} + V_{in2} \quad (5)$$

$$\frac{di_{L_f}}{dt} = \frac{V_{in1} + V_{in2} - V_o}{L_f} \quad (6)$$

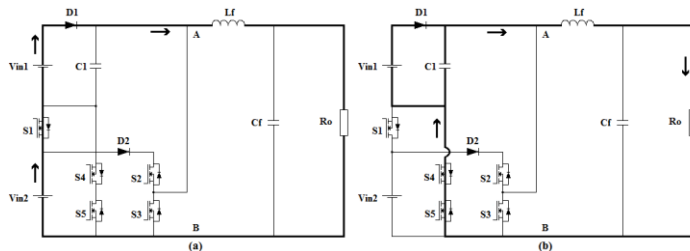


**Fig -3:** Equivalent circuit during (a) State III, (b) State IV

**State IV:** ( $S_4, S_5$  ON,  $S_1, S_2, S_3$  OFF)

Input source  $V_{in1}$  only deliver the power to the load. The voltage across the points A and B will be  $V_{in1}$  and it is more than  $V_o$ . Now the voltage appearing across the inductor  $L_f$  is  $(V_{in1} - V_o)$  and thereby the current  $i_{L_f}$  increases. Figure 3(b) shows the equivalent circuit during state IV.

$$v_{AB} = V_{in1} \quad (7)$$

$$\frac{di_{L_f}}{dt} = \frac{V_{in1} - V_o}{L_f} \quad (8)$$

**State V:** ( $S_2$  ON,  $S_1, S_3, S_4, S_5$  OFF)

Input source  $V_{in2}$  only supplies the power to the load. The voltage across the points A and B will be  $V_{in2}$  and it is less than  $V_o$ . Now the voltage appearing across the inductor  $L_f$  is  $(V_{in2} - V_o)$  and thereby the current  $i_{L_f}$  reduces. Figure 4(a) shows the equivalent circuit during state V.

$$v_{AB} = V_{in2} \quad (9)$$

$$\frac{di_{L_f}}{dt} = \frac{V_{in2} - V_o}{L_f} \quad (10)$$

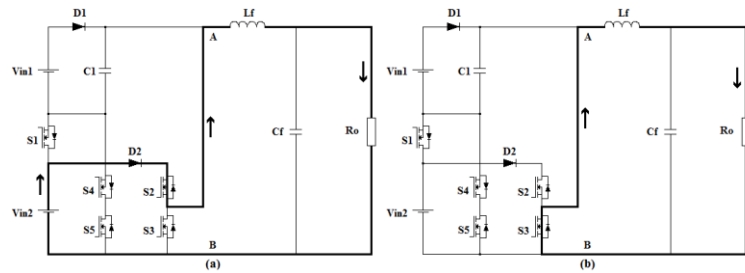


**Fig-4:** Equivalent circuit during (a) State V, (b) State VI

**State VI:** ( $S_3$  ON,  $S_1, S_2, S_4, S_5$  OFF)

Inductor current  $i_{L_f}$  freewheels through the switch  $S_3$  during this state. The voltage across the points A and B will be zero. The current  $i_{L_f}$  decreases. Figure 4(b) shows the equivalent circuit during state VI.

$$v_{AB} = 0 \quad (11)$$

$$\frac{di_{L_f}}{dt} = \frac{-V_o}{L_f} \quad (12)$$

Depending on the availability of the sources, their input voltages and power, the order of states during simultaneous operation will be states III, IV, VI or states III, V, VI. If more power is to be taken from the input source 1, state IV follows state III. In case more power is to be withdrawn from input source 2, state V follows state VI. -Figure 5(a) & (b) shows the waveforms related to mode I (simultaneous operation). Figure 6 presents the corresponding waveforms of mode II (bootstrap operation/individual operation).

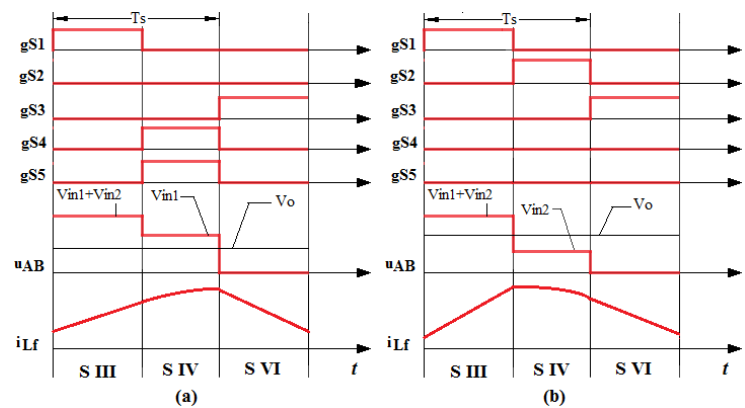


**Fig -5:** Waveforms during Mode I (simultaneous operation) with order of states (a) III, IV, VI, (b) III, V, VI

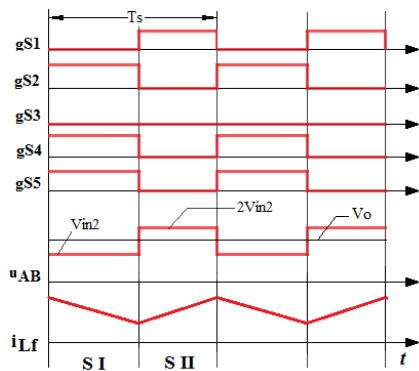


Fig -6: Waveforms during Mode II (Bootstrap operation)

across a switch is 80 V. Figure 10 shows the ripples in the output voltage waveform. Ripple percentage is seen as 1.51% of the average value.

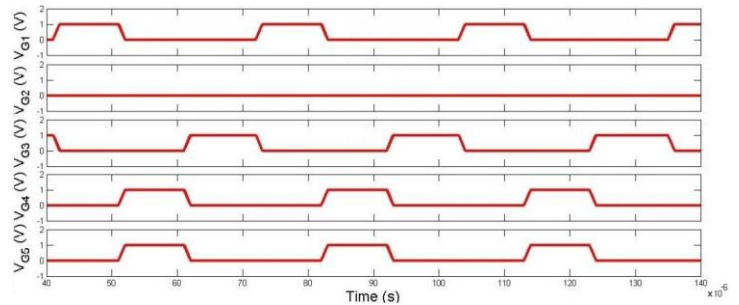


Fig -8: Mode I: Gate pulse voltages

### 3. SIMULATION MODELS AND RESULTS

The simulations were done on MATLAB/ Simulink R2014a. Figure 12 shows the simulink model of the converter.

Table -3: Simulation components, parameters and values

COMPONENT AND PARAMETERS	VALUE
Input Voltage 1 ( $V_{in1}$ )	50 V
Input Voltage 2 ( $V_{in2}$ )	30 V
Output Voltage ( $V_o$ )	40 V
Bootstrap Capacitor ( $C_1$ )	220 $\mu$ F
Filter Inductance ( $L_f$ )	400 $\mu$ H
Filter Capacitance ( $C_f$ )	300 $\mu$ F
Load Resistance ( $R_o$ )	2.2 k $\Omega$
Switching Frequency ( $f_s$ )	50 kHz

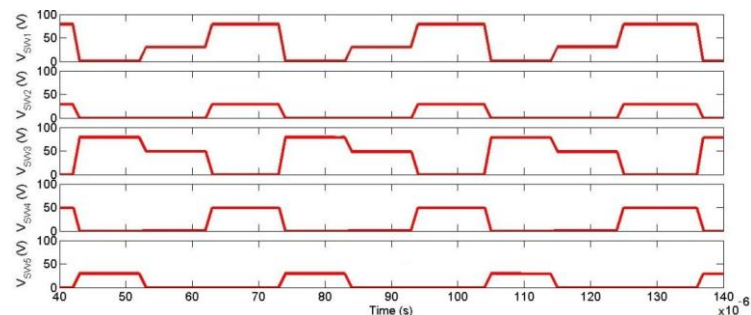


Fig -9: Mode I: Voltage stress across switches

Figure 7 shows the output voltage and current during the simultaneous operation, i.e., during mode I. The output voltage settles at 40 V.

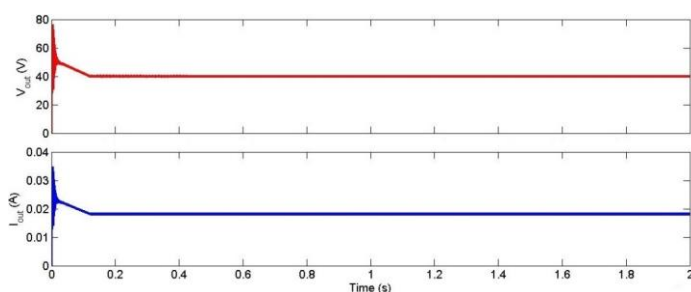


Fig -7: Output Voltage and Current when  $V_{in1}=50V$  and  $V_{in2}=30V$

Figure 8 shows the gate pulses to the converter switches during mode I. The voltage stresses across each of the switches are plotted in figure 9. The maximum voltage stress

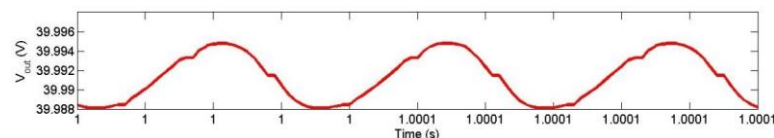


Fig -10: Mode I: Output voltage ripple

Figure 11 shows the output voltage and current during the bootstrap operation, i.e., during mode II. Although  $V_{in2}$  is only available, the output voltage is obtained as 40 V.

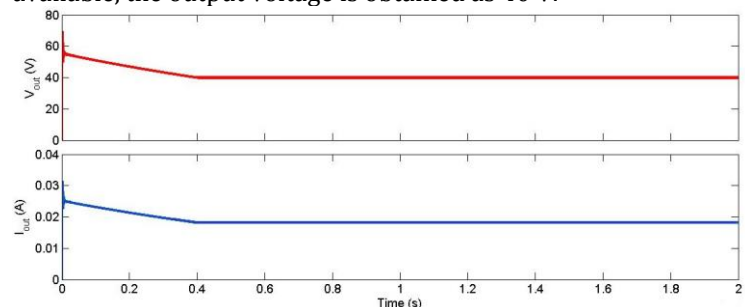


Fig -11: Mode II: Output Voltage and Current when  $V_{in1}=0V$  and  $V_{in2}=30V$

Figure 13 shows the gate pulses to the converter switches during mode I. The voltage stresses across the switches are plotted in figure 14. The maximum voltage stress across a switch is 50 V during this mode. Figure 15 shows the ripples in the output voltage waveform. Output voltage ripple is obtained as 0.042%



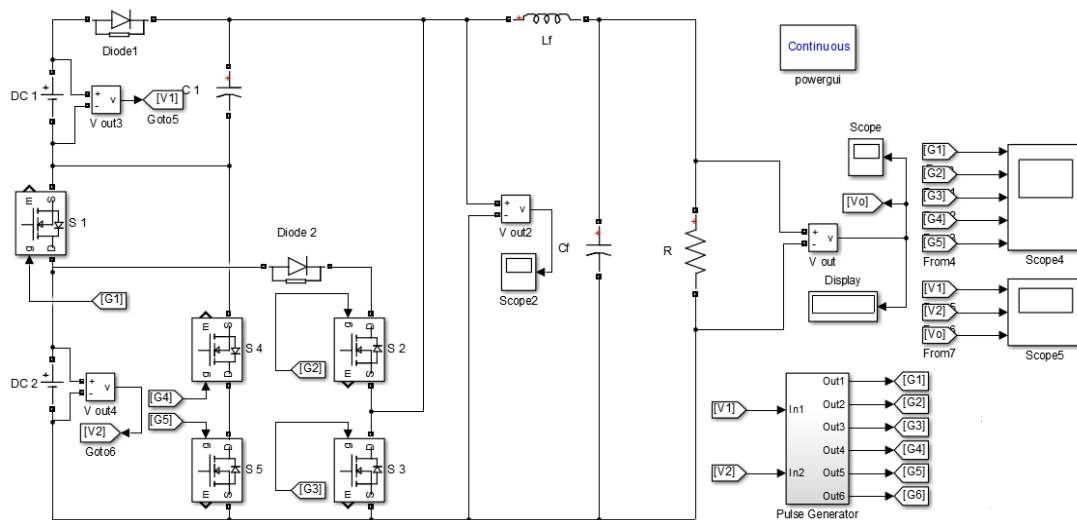


Fig -12: Simulink model of the DC-DC converter

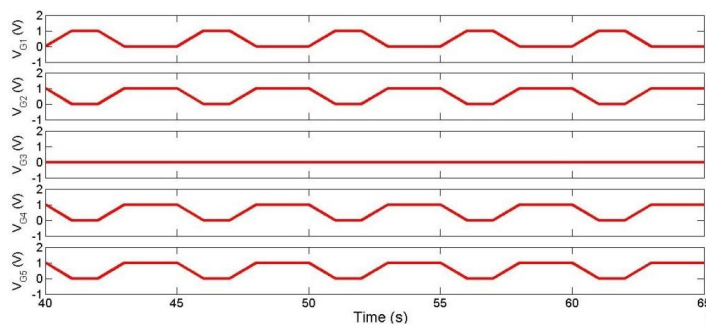


Fig -13: Mode II: Gate pulse voltages

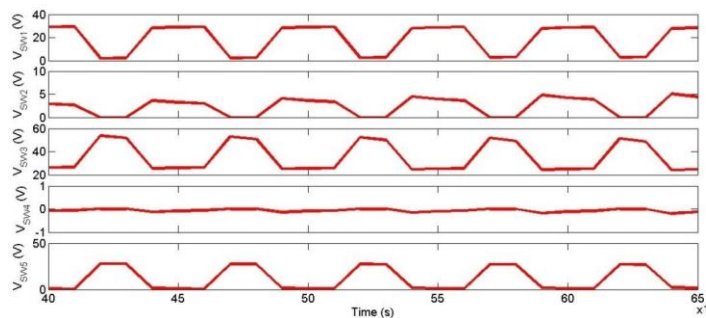


Fig -14: Mode II: Voltage stress across switches

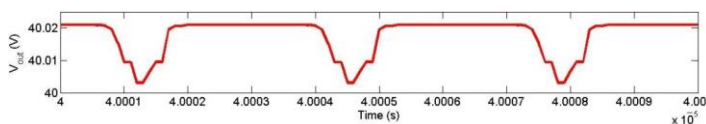


Fig -15: Mode II: Output voltage ripple

#### 4. CONCLUSIONS

The hybrid DC-DC converter for standalone applications is a simple and robust topology to solve the problems related to renewable energy source and ensure a constant output voltage. With the help of bootstrap operation, the fuel cell port can charge the renewable energy port if the renewable energy source is powered off from the circuit. This circuit contains only a single

inductor and there is no need for extra inductors while adding more input ports. This reduces the size and cost of the converter. Power density is improved and a good dynamic response is possible with this circuit. It is highly efficient during simultaneous and individual operation of the converter.

#### REFERENCES

- [1] K. Jin, X. Ruan, M. Yang and M. Xu, "A hybrid fuel cell power system," in *IEEE Transactions on Industrial Electronics*, vol. 56, no. 4, pp. 1212–1222, Apr.2009.
- [2] W. Jiang and B. Fahimi, "Active current sharing and source management in fuel-battery hybrid power system," in *IEEE Transactions on Industrial Electronics*, vol. 57, no. 2, pp. 752–761, Feb.2010.
- [3] L. Khanh, J. Seo, Y. Kim and D. Won, "Power management strategies for a grid connected PV-FC hybrid system," in *IEEE Transactions on Power Delivery*, vol. 25, no. 3, pp. 1874–1882, Jul.2010.
- [4] J. L. Duarte, M. A. M. Hendrix and M. G. Simoes, "Three-port bidirectional converter for hybrid fuel cell systems," in *IEEE Transactions on Power Electronics*, vol. 22, no. 2, pp.480–487, Mar. 2012.
- [5] C. Zhao, S.D. Round, and W. Johann, "An isolated three-port bidirectional DC-DC converter with decoupled power flow management", in *IEEE Transactions on Power Electronics*, vol. 23, no. 5, pp. 2443–2453, Sep.2008.
- [6] M. Sarhangzadeh, S. H. Hosseini, M. B. B. Sharifian, and G. B. Gharehpetian, "Multiinput direct DC-AC converter with high-frequency link for clean power generation systems," in *IEEE Transactions on Power Electronics*, vol. 26, no. 6, pp. 1777–1789, Jun.2011.
- [7] F. Nejabatkhah, S. Danyali, S. H. Hosseini, M. Sabahi, and S. M. Niapour, "Modeling and control of a new three-input dc-dc boost converter for hybrid PV/FC/battery power system," in *IEEE Transactions on Power Electronics*, vol. 27, no. 5, pp. 2309–2324, May 2012.
- [8] A. Khaligh, J. Cao, and Y. Lee, "A multiple-input DC-DC converter topology," in *IEEE Transactions on Power Electronics*, vol. 24, no. 3, pp. 862–868, Mar.2009.

- [9] Y. Li, D. Yang, and X. Ruan, "A new double-input DC-DC converter", in *Transactions of China Electrotechnical Society*, vol. 23, no. 6, pp. 77–82, Jun.2008.
- [10] Y. Li, X. Ruan, D. Yang, and F. Liu, "Interleaved dual-edge modulation scheme for double-input Buck converter", in *Transactions of China Electrotechnical Society*, vol. 24, no. 4, pp. 139–146, Apr.2009.
- [11] Y. Li, X. Ruan, D. Yang, and F. Liu, "Modeling and design of control system for double-input DC/DC converter", in *Transactions of China Electrotechnical Society*, vol. 25, no. 11, pp. 90–99, Nov.2010.
- [12] X. Sun, W. Wang, B. Wang and Z. Zhang, "Alternate source port tolerant series connected double input DC-DC converter," *IEEE Transactions on Power Electronics*, vol. 30, no. 5, pp.2733-2742, May 2015.